# Alma Mater Studiorum Università di Bologna
## Archivio istituzionale della ricerca

The Barrier to Proton Transfer in the Dimer of Formic Acid: A Pure Rotational Study

(Article begins on next page)

19 April 2024

# The Barrier to Proton Transfer in the Dimer of Formic Acid: A Pure Rotational Study

*Weixing Li, Luca Evangelisti, Qian Gou, Walther Caminati,\* and Rolf Meyer*

***Abstract:*** *The rotational spectra of three C-deuterated iso-topologues of the dimer of formic acid have been measured, thanks to the small dipole moment induced by asymmetric H → D substitution(s). For the DCOOH–HCOOH species, the concerted double proton transfer of the two hydroxy hydrogen atoms takes place between two equivalent minima and generates a tunneling splitting of 331.2(6) MHz. This splitting can be reproduced by a 3D model with a barrier of 2559 cm$^{-1}$ (30.6 kJ mol$^{-1}$) as obtained from theoretical calculations.*

$C$arboxylic acids form considerably stable dimers, that are sufficiently abundant at experimental conditions in a supersonic jet expansion. A number of molecular complexes involving carboxylic acids[1-10] have been investigated by rotational spectroscopy, to understand the nature of their non-covalent interactions and to have information on their internal dynamics and on their conformational equilibria. Much attention has been paid to the complexes of carboxylic acids, mainly to their dimers[1] and to their adducts with water.[2] Plenty of data have been obtained on the hydrogen-bonded dimers involving proton tunneling, the Ubbelohde effect and conformational equilibria.[1] HCOOH (formic acid; FA) is the prototype of the carboxylic acids family and for this reason it is involved in most of the investigations of carboxylic acids bonded to molecules containing other functional groups, such as its adducts with $H_2O$,[2a] $N(CH_3)_3$,[3] $CO_2$,[4] the simplest aldehyde $CH_2O$,[5] the simplest amide $H(CO)NH_2$,[6] ethers,[7] ketones,[8] freons,[9] azines[10] and its reactivity with alcohols.[11] An interesting feature of the dimer of FA, $(FA)_2$, is the concerted transfer of the two hydroxylic protons, a motion in a double minimum potential. It can generate tunneling doubling observable in molecular spectra, and makes them useful to studies of the tunneling process. The precise tunneling splittings ($\Delta E_{01}$) measured by microwave (MW) spectroscopy for the acrylic acid dimer[1g] and for the formic acid—benzoic acid bi-molecule[1h] have been reproduced by

[*] W. Li, L. Evangelisti, W. Caminati
Dipartimento di Chimica "G. Ciamician"
University of Bologna
Via Selmi 2, 40126 Bologna (Italy)
E-mail: walther.caminati@unibo.it

Q. Gou
School of Chemistry and Chemical Engineering, Chongqing University
Daxuecheng South Rd. 55, 401331, Chongqing (China)

R. Meyer
Sonnenbergstrasse 18, 5621 Zufikon (Switzerland)

model calculations with barriers at or close to values obtained ab initio.

In Figure 1 we show the proton transfer motion in the formic acid dimer along a symmetric double minimum potential energy profile.
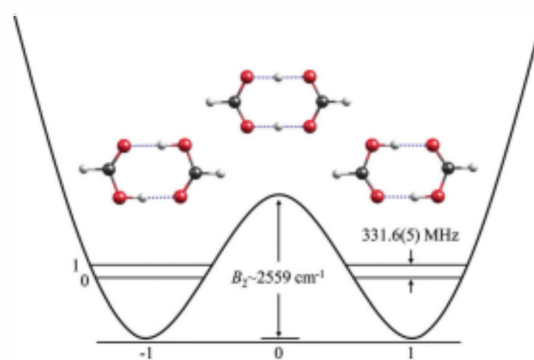


**Figure 1.** Proton transfer between equivalent forms of the formic acid dimer gives rise to a tunneling doublet for the vibrational ground state. The splitting measured by microwave experiments for the species DCOOH–HCOOH is given. It is related to the barrier height and to the interaction with non-reactive vibrational modes. C gray, O red, H white, D blue.

For $(FA)_2$, splittings are not available from MW spectroscopy due to the lack of a permanent electric dipole moment. The results obtained from other experimental techniques and from theoretical calculations have been summarized some years ago in a review by Birer and Havenith,[12] where the reported tunneling splittings range, rather disappointingly, from 0.013 to 111 cm$^{-1}$. Ortlieb and Havenith[13] obtained the value $\Delta E_{01} = 0.0158(4)$ cm$^{-1}$, for the ground state, from the vibration-rotation-tunneling spectrum of $(FA)_2$ in the C-O stretch region at 1221.0–1226.7 cm$^{-1}$.

More recently, Duan and his group measured the vibration-rotation-tunneling absorption spectra of $(FA)_2$ in the C-O stretch region at 1215–1240 cm$^{-1}$ using a rapid-scan tunable diode laser spectrometer in conjunction with a slit supersonic expansion, and reported $\Delta E_{01} = 0.01649(15)$ cm$^{-1}$.[14] Last year, the same group measured the rotationally resolved infrared spectra of different vibronic bands and supplied the value $\Delta E_{01} = 0.011367(92)$ cm$^{-1}$.[15] The discrepancy with the previous value seems to be attributable to strong local perturbations caused by the rotation-tunneling coupling between two nearby vibrational states.

Although these values are quite precise, they do not have the accuracy which is generally provided by MW spectroscopy. Is it then possible to apply MW to $(FA)_2$? Probably yes,

following the ideas of Bauder and collaborators, who reported the spectra of non-polar molecules (e.g. benzene, cyclobutane, *trans*-butadiene),[16] taking advantage of the small dipole moment induced by H→D asymmetric isotopic substitution. Such a method has never been applied to non-polar dimers.

We thought that, owing to the high stability (and then high concentration) of $(FA)_2$ in a supersonic jet, it would have been possible to observe the rotational spectra of asymmetrically D-substituted species, as indicated in Figure 2. This was indeed the case, and the results are reported below. According to the experimental values of the dipole moments associated to the H→D asymmetric isotopic substitution, a dipole moment of approximately 0.004 D is expected for such a dimer.
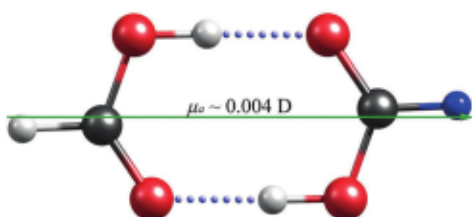


**Figure 2.** A small dipole moment of about 0.004 D is induced in DCOOH–HCOOH by H→D asymmetric substitution.

We applied this method for the first time to a non-polar molecular complex, investigating the rotational spectra of HCOOH-DCOOH and of two additional isotopologues. We succeeded in obtaining a precise experimental value of the $\Delta E_{01}$ values for the dimer of the non-polar adduct, by using Fourier transform microwave (MW) spectroscopy.

First, we ran some theoretical calculations[17] in order to calculate the spectroscopic parameters (e.g. D quadrupole coupling constants) reported in Table 1.

**Table 1:** B3LYP-D3/6–311 + + G(d,p) spectroscopic constants of HCOOH-DCOOH.

| | |
|---|---|
| $A$, $B$, $C$ [MHz] | 6051.7, 2218.7, 1623.5 |
| $D_J$, $D_{JK}$, $D_K$, $d_1$, $d_2$ [kHz] | 0.49, 6.2, 3.3, −0.14, −0.06 |
| $\chi_{aa}$, $\chi_{bb}-\chi_{cc}$ [MHz] | 0.19, 0.00 |

For the HCOOD–DCOOH and HCOOH–DCOOD species, we just mention here that the calculated values of $\chi_{aa}$ and $\chi_{bb}-\chi_{cc}$ for the OD deuterium are 0.20 and 0.00 MHz, respectively.

For molecular species with such a small dipole moment such as HCOOH–DCOOH a very high power of the MW pulses is required to polarize the sample, as described in the experimental section in the Supporting Information.

Our survey started with the search of the $K_{-1}=0$ $\mu_a$-transitions, which were expected to be more intense than the $K_{-1}>0$ ones. We could assign several of these transitions. The $2_{02} \leftarrow 1_{01}$ rotational transition was observed first. It was split into the two tunneling components $v=0$ (or $0^+$, symmetric) and $v=1$ (or $0^-$, antisymmetric), and each of them into two D
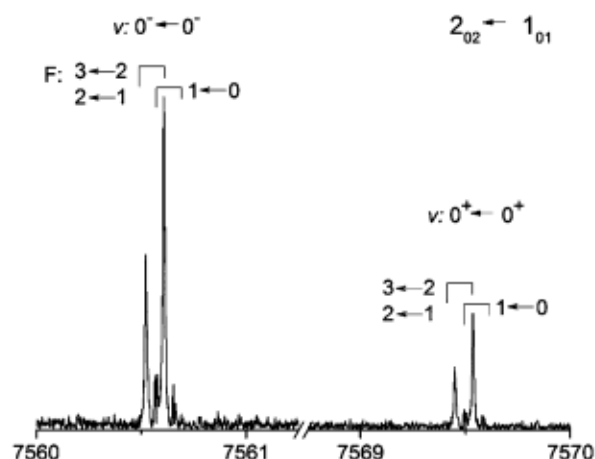


**Figure 3.** The $2_{02} \leftarrow 1_{01}$ rotational transition of DCOOH–HCOOH displaying the tunneling doublet, the related statistical weight, and the hyperfine structure arising from the D atom quadrupolar effects.

quadrupole component lines (see Figure 3), separated according to the quadrupole coupling constants given in Table 1.

It can be seen that for the ground state ($v=0$) the intensity of the transition ($K_{-1}=$ even) in Figure 3 is about 1/3 of that of $v=1$, while for transitions with $K_{-1}=$ odd, the reverse is observed. This is due to the statistical weight, as discussed ahead.

Many other $\mu_a$-type $R$-branch transitions have been measured, up to $J=5$ and $K_{-1}=2$. All transition frequencies (listed in the Supporting Information), have been fitted with Pickett's SPFIT program,[18] within the $I^r$-representation of Watson's $S$ reduction.[19]

The tunneling splittings were fitted using a two-state proton transfer-rotation coupled Hamiltonian, including semirigid rotor terms for each torsional state ($H_0^R$, $H_1^R$), common centrifugal distortion ($H^{CD}$) and D quadrupolar effects ($H^Q$), the torsional energy difference $\Delta E_{01}$, and the Coriolis coupling terms $F_{ab}$, according to Equation (1)

$$H = \begin{pmatrix} H_0^R + H^{CD} + H^Q & H_{int} \\ H_{int} & H_1^R + H^{CD} + H^Q + \Delta E_{01} \end{pmatrix} \quad (1)$$

with the interaction term given as Equation (2):

$$H_{int} = F_{ab}\ (P_aP_b + P_bP_a) \quad (2)$$

where $P_g$ ($g=a$ or $b$) are the angular momentum operators. The fitted spectroscopic constants for the two equatorial species are reported in Table 2.

Later on, the rotational spectrum of the DCOOH-HCOOD species has been investigated. In this case, the deuteration of a single OH group breaks down the symmetry of the complex, quenching the tunneling splitting and originating two different isotopologues (DCOO-D and HCOO-D, depending on the position of the D atom). Their spectra have been assigned, measured and fitted with a semirigid Watson Hamiltonian. The results are listed in Table 2.

**Table 2:** Spectroscopic constants of the three deuterated isotopologues.

| Parameter | DCOOH–HCOOH | | DCOOH–HCOOD | |
| --- | --- | --- | --- | --- |
| | $\nu=0$ | $\nu=1$ | HCOO-D | DCOO-D |
| $A$ [MHz] | 6038.65(8)[a] | | 5973.933(1) | 5972.996(1) |
| $B$ [MHz] | 2222.58(7) | 2222.55(7) | 2190.6557(7) | 2191.2593(7) |
| $C$ [MHz] | 1614.272(3) | 1614.238(3) | 1603.3693(5) | 1603.6217(5) |
| $D_J$ [kHz] | 0.757(7) | | 0.69(1) | 0.68(1) |
| $D_{JK}$ [kHz] | 3.40(6) | | 4.15(8) | 1.70(8) |
| $d_1$ [kHz] | −0.202(7) | | −0.20(1) | −0.21(1) |
| $\Delta E_{01}$ [MHz] | 331.6(5) | | | |
| $F_{ab}$ [MHz] | 299.1(4) | | | |
| $\chi_{aa}$(CD) [MHz] | 0.164(2) | | [0.19][b] | [0.19] |
| $\chi_{aa}$(OD) [MHz] | | | [0.20] | [0.20] |
| $\sigma$ [kHz][c] | 4.2 | | 3.0 | 4.3 |
| $N$[d] | 100 | | 36 | 38 |

[a] Error in parentheses in units of the last digit. [b] Numbers in brackets fixed at the ab initio value. [c] Root-mean-square deviation of the fit. [d] Number of lines in the fit.

The values $\chi_{bb}$-$\chi_{cc}$ were calculated to be 0.00 for both D(C-D) and D(O-D), and have been fixed to zero in the calculations.

We also tried to measure the spectrum of the DCOOD-HCOOD species, but the hyperfine structure due the multiple H→D substitutions was much more complex and the rotational lines much weaker, inhibiting a satisfactory observation of the spectrum.

As to the statistical weight, the $\nu=0$ and $\nu=1$ are symmetric or antisymmetric, respectively, with respect to the tunneling motions, and HCOOH–DCOOH has an effective $C_{2v}$ symmetry. The two hydroxy hydrogen atoms constitute a pair of equivalent fermions and then the molecular system follows the Fermi-Dirac statistics, that is, the overall wavefunction [Eq. (3)]

$$\psi_{tot} = \psi_e \psi_v \psi_R \psi_s \qquad (3)$$

must be anti-symmetric. The electronic wavefunction $\psi_e$ is symmetric (closed shell system), the vibrational wavefunctions $\psi_{v=0}$ and $\psi_{v=1}$ are symmetric and antisymmetric, respectively, while the spin function $\psi_s(3\,A_g; 1\,A_u)$ does have a ratio 3/1 between symmetric and anti-symmetric components. For this reason, for $\nu=0$ the rotational transitions with an anti-symmetric initial state $\psi_R$ will have a favorable intensity ratio of 3/1, with respect to the symmetric ones, and vice versa for symmetric initial state $\psi_R$. The contrary is true for $\nu=1$. With the $C_2$ symmetry axis lying along the $a$-axis, the even functions are characterized by an even value of $K_{-1}$, and vice versa.

In an attempt to help understanding the tunneling process in the formic acid dimer in terms of simple concepts we use a 3D flexible model that is supposed to simulate the most important properties. One of the earlier flexible model calculations[20] was made for a 2D hydrogen transfer system representing the collinear motion in I·H·I to study the Born-Oppenheimer type separation of the fast motion of the light hydrogen atom from the slow motion of the heavy Iodine atoms.[21] A 2D approach was also used to interpret the quantum dynamics of hydrogen transfer observed in crystals

of benzoic acid dimers.[22] In the case of the hydrogen transfer in malonaldehyde the role of heavy atom motions in the tunneling process had remained rather obscure despite many spectroscopic studies on this system. This was the motivation for a full dimensional quantum mechanical treatment[23] based on ab initio data able to reproduce the observed tunneling splittings. Yet the outcome was somewhat disappointing as the complexity of the results appeared to prevent insight into the most relevant interactions. Less extensive approaches were tried for the dimer of acrylic acid[1g] and of the adduct formic acid—benzoic acid.[1h] More recent work on the formic acid dimer is based on theoretical predictions for the full dimensional potential energy surface. The latter was used by Mackeprang et al.[24] for molecular dynamics calculations including hydrogen transfer to simulate the vibrational spectrum in the infrared. They were able to estimate the height of the barrier to hydrogen transfer by comparing simulated spectra obtained for models with different barrier heights with experimental spectra. Another very interesting full dimensional study presented by Richardson[25] is centered on the ground state tunneling splitting as derived from path integral methods and yielded a result close to the one obtained in the present work. It also lists the 1D result for the reactive mode and the successive increments or decrements found after including, one by one, all 23 non-reactive vibrational modes. As almost every mode appears to interact significantly it is prematurely proposed that a reduced-dimensionality model will not yield an accurate result.

While this might be true, it is hard to accept for someone used to microwave spectroscopy where some 100 observed rotational transition frequencies can be accurately reproduced by 11 parameters, each with a specified physical meaning (see Table 2). This prototypical situation offers the benefits of a substantial data reduction and of gaining insight into the properties of the system studied. Hydrogen transfer systems are different. As the tunneling splitting depends on many complex interactions, they suffer from a shortage of relevant experimental data and require support from theory that may deliver data that are not easily understood. So there is no longer a chance for data reduction and revealing model properties unless the information from theory is included along with the experimental data in an analysis trying to capture the most important properties of a simplified model. Therefore we insist that it is premature to reject a model that involves only 3 reduced coordinates referring to the 9 normal coordinates that will or may change when going from an equilibrium configuration to the saddle point. According to Richardson[25] these modes are numbered 1–9 and are of $A_g$ type with respect to the $C_{2h}$ symmetry of the parent species of the formic acid dimer. The reduced coordinates are $x$, $y_1$, $y_2$, have values 0, 0, 0 at the saddle point and ±1, ±1, +1 at the two equilibrium configurations. The variable $x$ describes the reactive mode 1 while $y_1$ and $y_2$ are used for collective "representative" non-reactive modes supposed to emulate the effects of Richardson's modes 3, 7 and 8 linked to $y_1$ and modes 2, 4, 5, 6, and 9 linked to $y_2$. Potential energy couplings between $x$ and the two $y$ variables will affect the tunneling process by their influence on the effective mass and on the accessible regions in configuration space.

To define these motions involved in the symmetric double minimum hydrogen transfer we use the two equivalent equilibrium structures and the saddle point configuration obtained by ab initio geometry optimization. The respective minimum energy path (MEP) is traced by the reduced coordinate $x$ describing the motion of the two hydrogen atoms and the cooperative heavy atom motions as functions of $x$. By definition the saddle point and the two minima of the potential energy correspond to the values $x = 0$ and $x = \pm 1$, respectively. To describe the concerted double hydrogen transfer we refer to the midline passing through the center between the C atoms, perpendicular to the C$\cdots$C direction, and within the symmetry plane. At $x = 0$ both hydrogen atoms are on this midline, and at $x = \pm 1$ they have travelled parallel to the C$\cdots$C axis but in opposite directions to the distance from the midline that they have at equilibrium. For a motion along the MEP, the variation of a structural parameter $S_i$ might then be approximated as $S_{ie}(x) = c_{i0} + c_{i1}x + c_{i2}x^2$ where the subscript $e$ indicates the restriction to the MEP. In order to partially relax the restriction to the MEP we replace $x$ and $x^2$ by reduced coordinates $y_1$ and $y_2$, respectively, and allow these to deviate from the MEP by independent vibrational displacements: $y_1 = x + \Delta y_1$ and $y_2 = x^2 + \Delta y_2$. Thus we arrive at the set of independent variables $(x, y_1, y_2)$ describing the 3D system. The antisymmetric changes of C–O and C=O bond lengths, associated with losing or gaining an OH bond, and the $A_g$ type rocking of the two $CO_2$ moieties are probably the most important modes of those related to $y_1$, and the dominant contribution to the collective motion related to $y_2$ is the change of the C$\cdots$C distance.

The present model involves an adaptable MEP in the $x$, $y_1$ space. Rather than using the first order approximation $y_{1e}(x) = x$ we choose another odd function [Eq. (4)]

$$y_{1e}(x) = (1 + a_1)x^3/(1 + a_1|x|^3) \quad (a_1 > 0). \tag{4}$$

Where the parameter $a_1$ allows one to modify the calculated tunneling splitting while leaving the barrier at or reasonably close to the value predicted ab initio. It implies that coupling of $y_1$ to $x$ is absent near $x = 0$, sets in near an equilibrium configuration ($x = \pm 1$) and levels off at large $|x|$. For the reduced coordinate $y_2$ we adopt the approximation $y_{2e}(x) = x^2$ up to a critical threshold $|x| = x_{crit}$. Its value ($x_{crit} \approx 1.533$) is given by the increment of the C$\cdots$C distance for a unit change of $y_2$ and on the increment of the H displacement along the C$\cdots$C direction for a unit change of $x$ [Eq. (5)]

$$\begin{aligned} y_{2e}(x) &= x^2 & (|x| \leq x_{crit}), \\ y_{2e}(x) &= x_{crit}(2|x| - x_{crit}) & (|x| > x_{crit}) \end{aligned} \tag{5}$$

According to this scheme for $|x| > x_{crit}$ the C and associated hydroxy H atoms travel the same distances in the same direction as expected for a separation of the two monomer moieties near their own equilibrium configuration.

The potential energy function is assumed to consist of the profile $V_{MEP}$ and the increments $V_1$ and $V_2$ arising when $y_1$ and $y_2$, respectively, deviate from their value on the MEP [Eq. (6)]

$$V(x, y_1, y_2) = V_{MEP}(x) + V_1(x, y_1) + V_2(x, y_2) \tag{6}$$

The first term [Eq. (7)]

$$V_{MEP}(x) = B_e(1 - x^2)^2/[1 + w\,(B_e/D_e)^{1/2}\,x^2 + (B_e/D_e)\,x^4], \tag{7}$$

contains the usual forth order expression with the barrier height $B_e$ and a denominator needed to shape the profile with its asymptotic approach to the dissociation energy $D_e$. In the present calculation both $B_e$ and $D_e$ are kept as obtained ab initio. The parameter $w$ allows one to modify the thickness of the barrier and the curvature in the potential minima and hence to also influence the deuteration effect on the calculated tunneling frequency. The increment arising from a deviation of $y_1$ from local equilibrium [Eq. (8)]

$$V_1(x, y_1) = f_1\,[y_1 - y_{1e}(x)]^2 \tag{8}$$

is based on the ab initio results obtained for $V$ at equilibrium $(x, y_1, y_2) = (1, 1, 1)$ and with displaced $y_1$, $(1, 1 \pm 0.5, 1)$, enabling one to derive the force constant factor $f_1$.

The last term in Equation (6) is dominated by the effect of changing the distance $R_{CC}$ between the two carbon atoms. Its general behavior was probed by ab initio calculations with the monomer constituents fixed at their own equilibrium configurations and remaining aligned while $R_{CC}$ was changed by small steps. The results suggested that the potential energy profile for $y_1 = x = 1$ agreed quite well with a Lennard-Jones potential, expressed by the reduced distance $\rho = R_{CC}/R_{CC,e}$ on a scale defined by the dissociation energy $D_e$ obtained ab initio. For general $x$ and $y_2$ we use the known linear function $R_{CC}(y_2)$ and the function $y_{2e}(x)$ from Equation (5) to find [Eq. (9)]

$$\rho = R_{CC}(y_2)/R_{CC}[y_{2e}(x)] \tag{9}$$

and replace the full dissociation energy by its remainder in a local equilibrium at the energy $V_{MEP}(x)$, which is elevated for $|x| \neq 1$ [Eq. (10)]

$$V_2(x, y_2) = [D_e - V_{MEP}(x)]\,[\rho^{-12} - 2\rho^{-6} + 1] \tag{10}$$

For the model represented in terms of the three variables, the wavefunctions are calculated in two steps. First, the variable $y_2$ that refers to the low energy mode, is kept fixed as a parameter while the two-dimensional system is solved for the wavefunctions $\phi(x, y_1; y_2)$ and $y_2$-dependent energy levels $\varepsilon(y_2)$ for low vibrational quantum numbers $v_x$, $v_1$ and both tunneling sublevels $s$ and $a$. Then, with equidistant $y_2$ values chosen in a suitable range, the function $\varepsilon_{00s}(y_2)$ is used as the potential energy function for the $y_2$ motion to obtain the respective vibrational factors $\chi(y_2)$ and the corresponding energy levels $E$. The product $\phi_{00s}(x, y_1; y_2)\,\chi_{0s}(y_2)$ is an approximation to the 3D wavefunction $\psi_{000s}(x, y_1, y_2)$ labeled by the three vibrational quantum numbers and the tunneling sublevel index. Correspondingly, the level $E_{0s}$ obtained for $v_2 = 0$ is an approximation for $E_{000s}$ that should be the more accurate the slower the $y_2$ motion relative to the $x$ and $y_1$ motions. By using the potential energy function $\varepsilon_{00a}(y_2)$ one finds along the same lines the approximation $E_{0a}$ for the higher sublevel and $E_{0a} - E_{0s}$ for the tunnel splitting in the

vibrational ground state. This is the quantity denoted in the spectroscopic description above by $\Delta E_{01}$.

As expected the results given in Table 3 are very similar for the two isotopic species. Owing to the adjustment of the parameter $a_1$ the calculated tunneling splitting for DCOOH–HCOOH is close to the observed value, and that for the

**Table 3:** Energy levels from model calculations for formic acid dimer.[a]

| Parameter | DCOOH–HCOOH | HCOOH–HCOOH |
|---|---|---|
| $E_{00s}$ [cm$^{-1}$] | 1355.84 | 1355.84 |
| $(\varepsilon_{01s}-\varepsilon_{00s})$ [cm$^{-1}$] | 357.19 | 357.19 |
| $(\varepsilon_{10s}-\varepsilon_{00s})^{[b]}$ [cm$^{-1}$] | 2354.49 | 2354.49 |
| $E_{0s}$ [cm$^{-1}$] | 66.69 | 67.12 |
| $E_{1s}-E_{0s}$ [cm$^{-1}$] | 140.71 | 141.53 |
| $E_{0a}-E_{0s}^{[c]}$ [MHz] | 331.28 | 334.89 |
| Parameters | | |
| $B_e$ [cm$^{-1}$] | 2559[d] | |
| $D_e$ [cm$^{-1}$] | 5267[d] | |
| $f_1$ [cm$^{-1}$] | 5292[d] | |
| $a_1/1$ | 0.6019[e] | |
| $w/1$ | 0[f] | |

[a] Levels denoted by $\varepsilon$ refer to the 2D subsystem at fixed $y_2 = 1$; their indices are the vibrational quantum numbers $v_x$, $v_1$ and the symmetry label $s$ or $a$ of the respective tunneling sublevel. Levels denoted by $E$ are relative to the value of $\varepsilon_{00s}(y_2 = 1)$. They refer to $v_x = v_1 = 0$ and $v_2 = 0$ or 1. [b] Estimated as $2 \times \varepsilon_{00s} - (\varepsilon_{01s} - \varepsilon_{00s})$. [c] Denoted as $\Delta E_{01}$ in the spectroscopic description; the value observed for DCOOH-HOOCH is 331.6 cm$^{-1}$. [d] From ab initio results. [e] Adjusted. [f] Assumed.

parent species HCOOH– is predicted to be higher by only about 4 MHz. From the zero-point energy $\varepsilon_{00s}$ obtained at fixed $y_2 = 1$ and the respective vibrational $y_1$ fundamental $\varepsilon_{01s}-\varepsilon_{00s}$ one estimates the zero point energy contribution by the transfer mode $x$ as $\varepsilon_{00s} - (\varepsilon_{01s} - \varepsilon_{00s})/2 = 1177$ cm$^{-1}$ and the first excited state $\varepsilon_{10s}$ of the $x$ vibration already well above the barrier. In Table 4 we show the model properties obtained by the present approach for the three similar systems studied in this laboratory.

**Table 4:** Properties of carboxylic acid adducts according to the present model.

| | Benzoic–Formic acid bimolecule Ref. [1h] | | Acrylic acid dimer cis-trans isomer Ref. [1g] | | Formic acid dimer DCOOH-HCOOH This work | |
|---|---|---|---|---|---|---|
| Parameters | | | | | | |
| $B_e$ [cm$^{-1}$] | 2595[a] | | 2328[b] | | 2559[b] | |
| $D_e$ [cm$^{-1}$] | 5475[b] | | 5642[b] | | 5267[b] | |
| $f_1$ [cm$^{-1}$] | 5030[b] | | 4936[b] | | 5292[b] | |
| $a_1/1$ | 0.30[c] | | 0.5355[a] | | 0.6019[a] | |
| $w/1$ | −1.19[a] | | −0.812[a] | | 0[c] | |
| Tunneling splittings $\Delta E_{01}$/ MHz | | | | | | |
| calc. | HH | 549.4 | HH | 880.6 | HH | 331.3 |
| obs. | | 548.7 | | 880.6 | | 331.6 |
| calc. | DD | 8.4 | HD | 114.3 | | |
| obs. | | 8.3 | | 117.0 | | |
| calc. | | | DH | 119.5 | | |
| obs. | | | | 117.1 | | |
| calc. | | | DD | 22.8 | | |
| obs. | | | | 31 | | |

[a] adjusted. [b] ab initio result. [c] assumed.

For all three systems the observed tunneling splittings can be reproduced with the ab initio results for the parameters $B_e$, $D_e$, $f_1$ and for the structures associated with the stationary points. It was sufficient to adjust one or both of the parameters $a_1$ and $w$ to reach agreement with observations. For the adduct of benzoic and formic acid and for the acrylic acid dimer the barrier shape parameter $w$ was needed to reproduce the observed effect of deuteration within the carboxy groups. But the assumption $w = 0$ had to be made for the formic acid dimer where an experimental tunneling splitting was not available for a hydroxy-deuterated species.

The current model with the parameters $a_1$ and $w$ refers to the MEP and, respectively, to the potential energy profile along the MEP. It still represents a tentative approach and should be tested by further applications, by studying the significance of the properties described, by comparison with alternatives and with quantum chemical results such as those reported by Richardson.[25] In his work the vibrational frequencies $\omega_f$ of the non-reactive modes are given at the potential energy minima and at the saddle point. From these one derives a zero-point vibrational energy $\frac{1}{2} \Sigma \omega_f$ higher by 115 cm$^{-1}$ at the saddle point than at equilibrium. This difference may be treated as an increment $\Delta B_0$ to the effective barrier height $B_0 = B_e + \Delta B_0$. In the sum of the frequency differences the largest term in absolute value comes from the $B_u$ type OH stretching mode, $\omega_{10,sad} - \omega_{10,min} = \Delta\omega_{10} = -2085$ cm$^{-1}$. The remaining 4 non-reactive modes dominated by motions of hydroxylic H atoms ($f = 6, 11, 12, 14$) contribute positive increments adding up to 1181 cm$^{-1}$. Hence the effect of all 5 non-reactive hydroxy H motions is predicted to lower the effective barrier by $\frac{1}{2}(-2085 + 1181) = -452$ cm$^{-1}$ for the parent species. This means that the contribution by the remaining non-reactive modes must be 567 cm$^{-1}$ to yield the total $567 - 452 = 115$ cm$^{-1}$. The contribution by the non-reactive modes not involving motions of hydroxylic H atoms is expected to be about the same after replacing the latter by deuterium, 567 cm$^{-1}$, but the negative overall contribution by the successors (after deuteration) of the modes $f = 6, 10, 11, 12, 14$ is estimated to be $(-452)/\sqrt{2} = -320$ cm$^{-1}$. So the predictions for the dimers (HCOOH)$_2$ and (HCOOD)$_2$ are found to be $\Delta B_0(HH) = 115$ cm$^{-1}$ and $\Delta B_0(DD) = 247$ cm$^{-1}$ with the difference $\Delta B_0(DD) - \Delta B_0(HH) = 132$ cm$^{-1}$ due to the interaction of the transfer mode with the 5 non-reactive hydroxylic modes. This difference could be introduced as a complement or an alternative to our shape parameter $w$ used for the benzoic acid–formic acid bimolecule and the acrylic acid dimer. Also the effects of coupling with skeletal modes on tunneling distances and splittings, that are contained in the ab initio data, should be explored in order to eventually arrive at the most significant model properties. Thus the detailed quantum chemical results from Ref. [25] may offer complementary or alternative information to test and improve our model.

In conclusion we note that this work reports the first rotational investigation of a non-polar adduct, the dimer of formic acid, the prototype of carboxylic acid dimers that undergo hydrogen transfer. In Table 5 we show our experimental tunneling splitting obtained from microwave (MW) spectra with values that resulted from infrared (IR) tech-

**Table 5:** $\Delta E_{01}$ values (MHz) obtained with other spectroscopic methods are compared to the MW result.

| MW | IR (Duan 2) | IR (Duan 1) | IR (Havenith) |
|---|---|---|---|
| 331.6(5)[a] | 341(3) | 495(5) | 474(12) |
| this work | Ref. [15] | Ref. [14] | Ref. [13] |

[a] This value is for the DCOOH–HCOOH isotopologue. For the non-polar parent species HCOOH–HCOOH the model calculations yield $\Delta E_{01} = 334.9$ MHz.

niques. According to this table the MW data are considerably more precise than those obtained with other techniques and not dependent on strong local perturbations caused by the rotation–tunneling coupling between two nearby vibrational states. Probably the interpretation of this effect explains the marked difference between the two values reported by the Duan group. A relatively simple interpretation of the tunneling process on the basis of experimental data and a growing amount of ab initio information has been proposed by devising a 3D flexible model that might be worth being developed further.

## Acknowledgements

## Conflict of interest

The authors declare no conflict of interest.

[1] a) C. C. Costain, G. P. Srivastava, *J. Chem. Phys.* **1961**, *35*, 1903–1904; b) E. M. Bellott, Jr., E. B. Wilson, *Tetrahedron* **1975**, *31*, 2896–2898; c) L. Martinache, W. Kresa, M. Wegener, U. Vonmont, A. Bauder, *Chem. Phys.* **1990**, *148*, 129–140; d) S. Antolinez, H. Dreizler, V. Storm, D. H. Sutter, J. L. Alonso, *Z. Naturforsch. A* **1997**, *52a*, 803–806; e) A. M. Daly, K. O. Douglass, L. C. Sarkozy, J. L. Neill, M. T. Muckle, D. P. Zaleski, B. H. Pate, S. G. Kukolich, *J. Chem. Phys.* **2011**, *135*, 154304; f) M. C. D. Tayler, B. Ouyang, B. J. Howard, *J. Chem. Phys.* **2011**, *134*, 054316; g) G. Feng, L. B. Favero, A. Maris, A. Vigorito, W. Caminati, R. Meyer, *J. Am. Chem. Soc.* **2012**, *134*, 19281–19286; h) L. Evangelisti, P. Ecija, E. J. Cocinero, F. Castaño, A. Lesarri, W. Caminati, R. Meyer, *J. Phys. Chem. Lett.* **2012**, *3*, 3770–3775; i) G. Feng, Q. Gou, L. Evangelisti, Z. Xia, W. Caminati, *Phys. Chem. Chem. Phys.* **2013**, *15*, 2917–2922; j) Q. Gou, G. Feng, L. Evangelisti, W. Caminati, *J. Phys. Chem. Lett.* **2013**, *4*, 2838–2842; k) Q. Gou, G. Feng, L. Evangelisti, W. Caminati, *J. Phys. Chem. A* **2013**, *117*, 13500–13503; l) Q. Gou, G. Feng, L. Evangelisti, W. Caminati, *Chem. Phys. Lett.* **2014**, *591*, 301–305; m) G. Feng, Q. Gou, L. Evangelisti, W. Caminati, *Angew. Chem. Int. Ed.* **2014**, *53*, 530–534; *Angew. Chem.* **2014**, *126*, 540–544; n) L. Evangelisti, G. Feng, Q. Gou, W. Caminati, *J. Mol. Spectrosc.* **2014**, *299*, 1–5; o) Q. Gou, G. Feng, L. Evangelisti, W. Caminati, *ChemPhysChem* **2014**, *15*, 2977–2984.

[2] a) D. Priem, T.-K. Ha, A. Bauder, *J. Chem. Phys.* **2000**, *113*, 169–175; b) see, for example, B. Ouyang, B. J. Howard, *Phys. Chem. Chem. Phys.* **2009**, *11*, 366–373; c) B. Ouyang, T. G. Starkey, B. J. Howard, *J. Phys. Chem. A* **2007**, *111*, 6165–6175; d) B. Ouyang, B. J. Howard, *J. Phys. Chem. A* **2010**, *114*, 4109–4117; e) E. G. Schnitzler, W. Jäger, *Phys. Chem. Chem. Phys.* **2014**, *16*, 2305–2314; f) E. G. Schnitzler, B. L. M. Zenchyzen, W. Jager, *Phys. Chem. Chem. Phys.* **2016**, *18*, 448–457; g) G. Feng, Q. Gou, L. Evangelisti, L. Spada, S. Blanco, W. Caminati, *Phys. Chem. Chem. Phys.* **2016**, *18*, 23651–23656.

[3] R. B. Mackenzie, C. T. Dewberry, K. R. Leopold, *J. Phys. Chem. A* **2016**, *120*, 2268–2273.

[4] A. Vigorito, Q. Gou, C. Calabrese, S. Melandri, A. Maris, W. Caminati, *ChemPhysChem* **2015**, *16*, 2961–2967.

[5] Q. Gou, L. B. Favero, S. S. Bahamyirou, Z. Xia, W. Caminati, *J. Phys. Chem. A* **2014**, *118*, 10738–10741.

[6] A. M. Daly, B. A. Sargus, S. G. Kukolich, *J. Chem. Phys.* **2010**, *133*, 174304.

[7] L. Evangelisti, L. Spada, W. Li, A. Ciurlini, J.-U. Grabow, W. Caminati, *J. Phys. Chem. A* **2016**, *120*, 2863–2867.

[8] L. Evangelisti, L. Spada, W. Li, S. Blanco, J. C. Lopez, A. Lesarri, J.-U. Grabow, W. Caminati, *Phys. Chem. Chem. Phys.* **2017**, *19*, 204–209.

[9] Y. Jin, J. Wang, Q. Gou, Z. Xia, G. Feng, *Spectrochim. Acta Part A* **2019**, *206*, 185–189.

[10] L. Spada, Q. Gou, B. M. Giuliano, W. Caminati, *J. Phys. Chem. A* **2016**, *120*, 5094–5098.

[11] L. Evangelisti, L. Spada, W. Li, F. Vazart, V. Barone, W. Caminati, *Angew. Chem. Int. Ed.* **2017**, *56*, 3872–3875; *Angew. Chem.* **2017**, *129*, 3930–3933.

[12] O. Birer, M. Havenith, *Annu. Rev. Phys. Chem.* **2009**, *60*, 263–275.

[13] M. Ortlieb, M. Havenith, *J. Phys. Chem. A* **2007**, *111*, 7355–7363.

[14] K. G. Goroya, Y. Zhu, P. Sun, C. Duan, *J. Chem. Phys.* **2014**, *140*, 164311.

[15] Y. Zhang, W. Li, W. Luo, Y. Zhu, C. Duan, *J. Chem. Phys.* **2017**, *146*, 244306.

[16] a) M. Oldani, A. Bauder, *Chem. Phys. Lett.* **1984**, *108*, 7–10; b) B. Vogelsanger, W. Caminati, A. Bauder, *Chem. Phys. Lett.* **1987**, *141*, 245–250; c) W. Caminati, G. Grassi, A. Bauder, *Chem. Phys. Lett.* **1988**, *148*, 13–16; d) W. Caminati, B. Vogelsanger, R. Meyer, G. Grassi, A. Bauder, *J. Mol. Spectrosc.* **1988**, *131*, 172–184.

[17] M. J. Frisch, G. W. Trucks, H. B. Schlegel, G. E. Scuseria, M. A. Robb, J. R. Cheeseman, G. Scalmani, V. Barone, G. A. Petersson, H. Nakatsuji et al. Gaussian 09 Revision D.01; Gaussian Inc.: Wallingford, CT, **2016**.

[18] H. M. Pickett, *J. Mol. Spectrosc.* **1991**, *148*, 371–377.

[19] J. K. G. Watson in *Vibrational Spectra and Structure*, Vol. 6 (Ed.: J. R. Durig), Elsevier, New York, **1977**, pp. 1–89.

[20] R. Meyer, *J. Mol. Spectrosc.* **1979**, *76*, 266–300.

[21] J. Manz, R. Meyer, E. Pollak, J. Römelt, *Chem. Phys. Lett.* **1982**, *93*, 184–187.

[22] a) R. Meyer, R. R. Ernst, *J. Chem. Phys.* **1990**, *93*, 5518–5532; b) A. Stöckli, B. H. Meier, R. Kreis, R. Meyer, R. R. Ernst, *J. Chem. Phys.* **1990**, *93*, 1502–1520.

[23] a) R. Meyer, T.-K. Ha, *Mol. Phys.* **2003**, *101*, 3263–3276; b) R. Meyer, T.-K. Ha, *Mol. Phys.* **2005**, *103*, 2687–2698.

[24] K. Mackeprang, Z.-H. Xu, Z. Maroun, M. Meuwly, H. G. Kjaergaard, *Phys. Chem. Chem. Phys.* **2016**, *18*, 24654–24662.

[25] J. O. Richardson, *Phys. Chem. Chem. Phys.* **2017**, *19*, 966–970.